

Original papers

Next-generation high-throughput phenotyping with trait prediction through adaptable multi-task computational intelligence

Jan Zdrazil^{a,b}, Lingping Kong^b, Pavel Klimeš^a, Francisco Ignacio Jasso-Robles^a,
 Iñigo Saiz-Fernández^a, Firat Güder^{c,d}, Lukáš Spíchal^a, Václav Snášel^{b,*}, Nuria De Diego^{a,*}

^a Czech Advanced Technology and Research Institute (CATRIN), Palacký University Olomouc, Šlechtitelů 27, 77900 Olomouc, Czech Republic

^b Faculty of Electrical Engineering and Computer Science, VSB-Technical University of Ostrava, Ostrava, Czech Republic

^c Department of Bioengineering, Imperial College London, London SW7 2AZ, UK

^d Bezos Centre for Sustainable Protein, Imperial College London, London, SW7 2AZ, United Kingdom



ARTICLE INFO

Keywords:

Fast testing and analysis
 General purposes
In vitro culture
 Machine learning
 Phenotyping markers
 Plant phenotyping

ABSTRACT

Phenotypes, which define an organism's behaviour and physical attributes, result from the complex interplay of genetics, development, and environment. Predicting future plant traits is mainly challenging due to these dynamic interactions. This work presents AMULET, a modular approach that combines imaging-based high-throughput phenotyping and machine learning to predict morphological and physiological plant traits hours to days before they are visible. Trained with over 30,000 *Arabidopsis thaliana* plants, AMULET streamlines the phenotyping process by integrating plant detection, prediction, segmentation, and data analysis, enhancing workflow efficiency and reducing time. AMULET achieved impressive performance metrics, including a dice loss of 0.0104 and an IoU score of 0.9948 for the test set, indicating high accuracy in the segmentation task or an R^2 score of 0.9289 for descriptor estimation. Moreover, Simpler yet Better Video Prediction (SimVP) appeared as the most effective model in predicting plant growth and health status. Using phenotyping images from studies focused on the *Arabidopsis thaliana*-*Pseudomonas syringae* pathosystem, AMULET analysed the latent *phenom* by identifying traits restrictive to human perception and essential to understanding plant response to concrete growth conditions. Techniques like TorchGrad and Gradient-weighted Class Activation Mapping helped to reveal these new hidden traits. AMULET also demonstrated its adaptability by accurately detecting and predicting phenotypes of *in vitro* potato plants after minimal fine-tuning with just 100 plants. This versatile approach streamlines phenotyping and holds significant promise for improving breeding programs and agricultural management by enabling pre-emptive interventions optimising plant health and productivity.

1. Introduction

Although the genome codes an organism's potential trait, phenotypes are the real endpoint characteristics that determine an organism's behaviour and physical attributes at any given time (Chitwood and Topp, 2015; Kovach and McCouch, 2008). Unlike the well-defined, indivisible nature of genes, phenotypes are infinitely variable, influenced by genetics, developmental stage, and environment. This complexity is magnified by the enormous genetic diversity in the biological world, further expanded by the new genotypes obtained by traditional and modern breeding practices (Kovach and McCouch,

2008).

Humans rely on plants directly, as they constitute 80 % of the global diet, 29 % of the textile fibres (Townsend, 2020) and 11 % of building materials (Aytekin and Mardani-Aghabaglou, 2022) or indirectly, as a source of energy and oxygen and through the consumption of plant-eating animals as a source of food (<https://www.fao.org/plant-health-2020/home/en/>). Breeding to modify specific phenotypic traits is challenging due to the diverse environmental conditions that crops face during their life cycle, affecting everything from germination to yield (Lippmann et al., 2019). Consequently, selecting desirable phenotypes is a numbers game hindered by a fundamental lack of biological

* Corresponding authors.

E-mail addresses: jan.zdrazil@upol.cz (J. Zdrazil), lingping.kong@vsb.cz (L. Kong), pavel.klimes@upol.cz (P. Klimeš), franciscoignacio.jassorobles@upol.cz (F.I. Jasso-Robles), inigo.saizfernandez@upol.cz (I. Saiz-Fernández), guder@ic.ac.uk (F. Güder), lukas.spichal@upol.cz (L. Spíchal), vaclav.snasel@vsb.cz (V. Snášel), nuria.de@upol.cz (N. De Diego).

<https://doi.org/10.1016/j.compag.2025.110390>

Received 4 February 2025; Received in revised form 12 March 2025; Accepted 5 April 2025

Available online 12 April 2025

0168-1699/© 2025 The Authors. Published by Elsevier B.V. This is an open access article under the CC BY license (<http://creativecommons.org/licenses/by/4.0/>).

understanding. Therefore, it is essential to test many genotypes under various conditions to find the ones that produce the desired phenotypes efficiently.

High-Throughput Phenotyping (HTP) is an advanced method combining imaging, robotics, and sensor networks to collect big datasets from large plant populations (Fiorani and Schurr, 2013; Roupael et al., 2018). An advanced HTP setup can analyse over 25,000 plants in one run (De Diego et al., 2017), facilitating significant breakthroughs in identifying and characterising biostimulants (Sorrentino et al., 2021; Ugena et al., 2018), eco-friendly agrochemicals (Bryksova et al., 2020), and genotypes with improved resilience (Jasso-Robles et al., 2024). Combined with other –omics, HTP also enables an understanding of plant responses to multifactorial stress conditions (Vrobel et al., 2024).

Arabidopsis thaliana, a Brassicaceae family member, is the most used model organism in plant research worldwide because of its well-characterised genome, ease of cultivation and manipulation, short life cycle, and prolific seed production plant (Koorneef and Meinke, 2010). Despite the capability of miniaturising HTP technologies using *Arabidopsis* as a model plant, the challenge remains in segmenting these tiny plants (2–4 mm diameter of four-day-old seedling) at earlier developmental stages. Furthermore, analysing and interpreting these complex datasets is time-consuming and requires advanced statistical and computational techniques beyond traditional methods.

For more efficient use of the big data obtained from HTP experiments, tasks such as plant detection, segmentation, and data analysis are crucial for identifying the most relevant characteristics related to plant resilience. Moreover, current phenotyping approaches remain limited by human-defined attributes of what constitutes a phenotype. Traditionally, we perceive phenotypes as measurable, human-interpretable traits—such as height, leaf area, or colour—but using new analytic approaches, such as integrating artificial intelligence (AI), allows transcending these predefined categories. Rather than restricting the phenotype to human-perceived traits, AI will enable us to explore the *phenom*—the full spectrum of phenotypic expression, including both observable and latent traits shaped by genetics, environment, and developmental factors. This concept expands beyond conventional definitions, viewing phenotype not as a static set of measurable characteristics but as a dynamic and emergent space where novel patterns, relationships, and biological insights can be uncovered. By exploring the latent space of the *phenom*, AI can reveal previously unrecognised features that may be biologically significant but are not readily apparent through conventional phenotyping.

The integration of machine learning (ML) with big datasets from HTP is revolutionising the analysis of complex data from plants grown under different conditions (Anshori et al., 2023; Walsh et al., 2024). Imaging and ML technologies have proven effective in detecting and classifying plant diseases (Bhugra et al., 2024; Walsh et al., 2024) and response to specific abiotic stressors (Isak et al., 2024; Mertens et al., 2023; Zhai et al., 2023). Regardless of the sophistication of the current approaches offering identification of desirable traits related to plant resistance (Harfouche et al., 2023), most works focus on a single task such as classifying genotypes or diseases, plant segmentation, or stomata analysis (Gibbs and Burgess, 2024; Harfouche et al., 2023; Singh et al., 2021; Yuan et al., 2023). In other words, current approaches lack versatility as they are tailored to specific procedures or plant species. General-purpose models that can easily be fine-tuned across various experimental pipelines to enhance the versatility of analysis are, therefore, the “holy grail” of plant phenotyping. Moreover, many studies combining ML with plant phenotyping rely on sophisticated and costly non-invasive sensors [fluorescence, thermal, or hyperspectral cameras (Mertens et al., 2023; Son et al., 2024; Zhai et al., 2023)], which may not be accessible to all researchers and growers. Furthermore, there is a notable gap in predictive analytics, offering models with substantial potential for forecasting plant changes before they become apparent.

In this study, we introduce AMULET- Adaptable and MUlti-task machine Learning for Endless phenotyping Trait prediction- the next

generation in HTP technology (Fig. 1), which combines simple RGB imaging with AI-driven models for predicting morphological and physiological traits hours to days before their visible manifestation. This modular pipeline integrates plant detection, segmentation, prediction, and data analysis, making it readily adaptable for monitoring and predicting plant growth and stress response in different plant species. Fully compliant with REFORMS (REcommendations FOR Machine-learning-based Science) guidelines (Kapoor et al., 2024), AMULET transcends traditional computer vision tools by using longitudinally acquired plant imagery for a comprehensive range of tasks within a unified pipeline (Fig. 1), which constitutes a significant advancement in plant phenotyping, enhancing both its efficiency and impact, thereby supporting the development of more resilient plants and sustainable, productive agricultural practices.

2. Results and discussion

2.1. Workflow of AMULET

The AMULET workflow (Fig. 2 and Supplementary Fig. S1) starts with the automated capture of high-resolution RGB images of *Arabidopsis thaliana* plants grown *in vitro* into well-plates of varied sizes at the Olophen system (https://www.plant-phenotyping.org/db_infrastructure#/tool/57), a plant phenotyping platform equipped with PlantScreen™ XYZ and Compact systems (Photo System Instruments, PSI, Czech Republic). The HTP screening method uses the high-resolution top-view RGB camera to track *Arabidopsis* growth meticulously over 7 to 10 days (De Diego et al., 2017; Ugena et al., 2018). This process involves imaging the plants grown on multi-well plates at different developmental stages to generate a comprehensive training dataset. The main focus was studying plant-pathogen interaction using the *Arabidopsis thaliana*-*Pseudomonas syringae* (*Arabidopsis-Pst*) pathosystem as a model to demonstrate AMULET’s capabilities.

AMULET integrates a complex workflow of six stages, including plant imaging, object *detection*, time series *prediction*, image *segmentation*, and *evaluation* through the estimation of plant descriptors, culminating in a validation process (Fig. 2 and Supplementary Fig. S1). Initially, we preprocessed all datasets to standardise image size, enhancing the training and predictive accuracy of our ML models. This standardisation is crucial for analysing small targets such as early-stage *Arabidopsis* plants or minor leaf lesions formed in response to the pathogen.

2.2. Machine learning models for different modules of the AMULET pipeline

The processed images are analysed using a Faster Region-based Convolutional Neural Network (R-CNN) model (Ren et al., 2017) to ensure accurate object *detection* (Fig. 2 and Supplementary Fig. S1). This model improves traditional structures by incorporating modifications to the feature extractor, anchor ratios, region of interest pooling, and loss functions, specifically tailored to detect the specific characteristics of plant disease and phenotype traits effectively (Shoaib et al., 2023). Using over 32,000 *Arabidopsis* plants, our ML model has been trained to ensure precise detection across all types of multi-well plates (Supplementary Table S1). Such universal automatic and accurate detection for all multi-well plates is crucial to ensure each plant is correctly identified and prepared for subsequent analysis.

To maintain positional consistency across different time points and plate distributions, we have developed a robust validation system that assigns a unique identifier to each plant (For more details, see Supplementary Fig. S2 and Subsection- Data preprocessing). This mechanism allows for precise tracking of individual plants over time, linking them with a database of previous measurements [Supplementary material- Algorithm 1 (“Validation of Plant Positions”)].

Fast R-CNN excels in object detection and is computationally

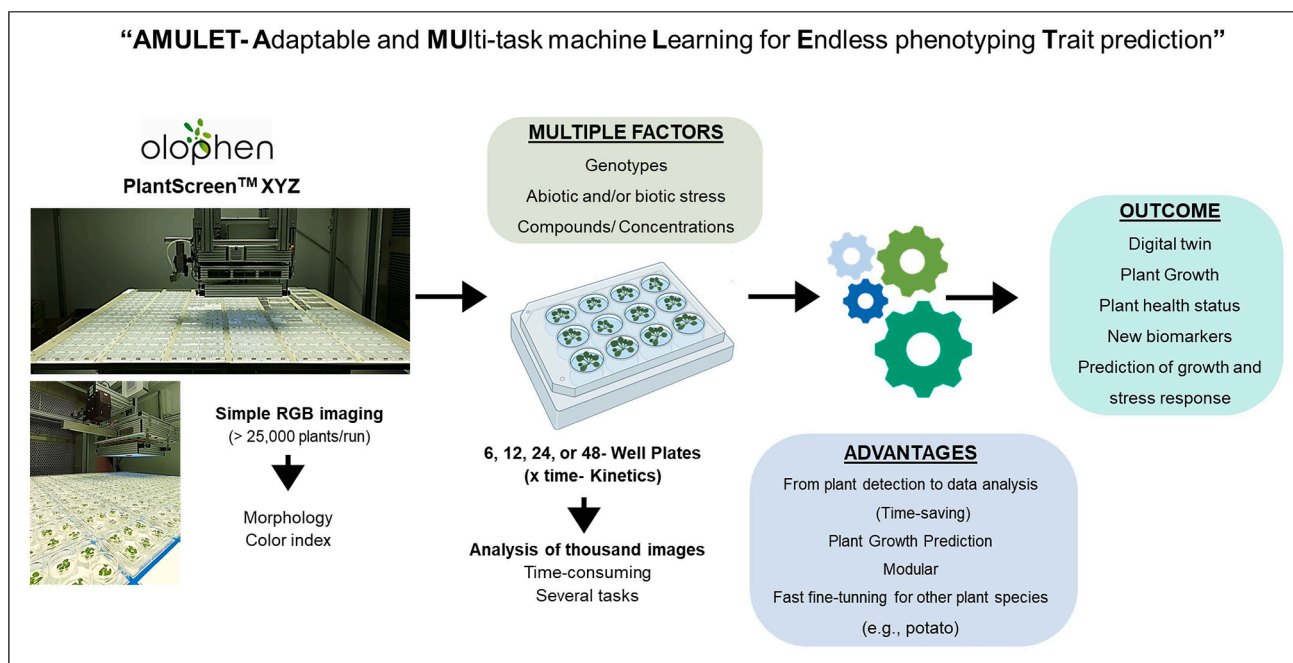


Fig. 1. AMULET- Adaptable and MULTI-task machine Learning for Endless phenotyping Trait prediction- pipeline involves different modules, starting with plant imaging using an RGB camera and then selecting different machine learning models for plant detection, prediction, segmentation, and data analysis. The advantages and outcomes are indicated.

efficient (Su et al., 2021; Xu et al., 2022), which is essential for accurately identifying small Arabidopsis plants. While the Faster R-CNN model is widely used for disease identification across various plant species (Zhou et al., 2023), it has limitations in detecting small objects. To address this, we supplemented it with other models to efficiently increase identification, particularly for three-day-old Arabidopsis seedlings (see **Subsection- Plant detection**).

The sequential imagery feeds into an image *prediction* model that forecasts the future appearance of each plant based on historical data (Fig. 2). This predictive capability is essential for understanding plant growth patterns and potential future states. To achieve this, we integrated more than 3,000 Arabidopsis seedlings imaged at six consecutive time points into the model. The images were obtained from a modified HTP screening method based on De Diego et al. (2017) to study Arabidopsis-*Pst* interaction. Our innovative non-invasive screening approach involved dropping bacterial suspension onto the leaves of two-week-old Arabidopsis seedlings, allowing a natural infection process (without infiltration) in which bacteria grow epiphytically (they can live and multiply on the outside of aerial surfaces of plants) and enter the plant through the stomata (Xin and He, 2013). Images were automatically captured before infection (t_0) and at intervals from 3 to 24 h post-inoculation (hpi) (from t_1 to t_6).

We selected the Simpler yet Better Video Prediction (SimVP) (Gao et al., 2022) model for plant *prediction* because it is skilled at handling temporal image sequences. This model was compared against other leading models such as TAU (Tan et al., 2023), ConvLSTM (Shi et al., 2015), and PredRNNv2 (Lee and Lee, 2024; Wang et al., 2017) to ensure its suitability for our data temporal complexity (for further details, see **Supplementary Table S3**). Remarkably, SimVP predicted the appearance of infection symptoms two-time points ahead, efficiently detecting infections in Arabidopsis seedlings at 9 hpi before they became visible to the naked eye at 24 hpi (Fig. 2 and **Supplementary Fig. S1, Movie S1**). This model is rarely used in Natural Sciences (Han et al., 2023) and even less in Plant Science. It was only recently used to predict disease in *Ginkgo biloba* leaves at more advanced developmental stages when the damage in the tissue was already evident (Yao et al., 2024). We demonstrated that the SimVP model was able to predict the progression

of the leaves of young Arabidopsis seedlings infected with *Pst* inoculation 15 h before the lesions were visible, corroborating it as a very robust model suitable for retraining to predict changes in the growth of other plant species.

Following prediction, the images underwent *segmentation* to isolate Arabidopsis rosette from the background, ensuring that subsequent analyses focus solely on plants free from background noise. We selected the pre-trained DeepLabV3+ (Chen et al., 2018) model integrated with an EfficientNet-B7 encoder after extensive testing with alternative encoders such as ResNet50 and ResNet101 (Fig. 2 and **Supplementary Fig. S1**). The EfficientNet-B7 stood out for its superior performance (Harkat et al., 2020; Zafar et al., 2023), ensuring precise segmentation for subsequent phases of our pipeline. Due to the small size of both Arabidopsis seedlings and the lesions induced by *Pst* in this very early stage of colonisation, selecting this method proved to be crucial, as it enabled precise image segmentation, especially in our setup for accurately evaluating the image to define organ or plant tissue that will be used for further analysis (**Supplementary Fig. S1**). This task model, trained on a diverse dataset comprising over 4,000 images of Arabidopsis plants grown in well-plates, offered invaluable depth of pattern recognition. It avoided recognizing artefacts, reaching a precise plant segmentation, even for small objects (**Supplementary Fig. S1**). The DeepLabV3 + model has demonstrated strong performance, corroborated by its success in detecting plants and identifying various diseases across multiple plant species (Li et al., 2022, 2023; Mahmood and Alsalem, 2024; Sharma and Sethi, 2024). The EfficientNet encoders have also performed well in disease classification (Polly and Devi, 2024). However, to date, only one study has paired the DeepLabV3 + with the EfficientNet encoder as part of the more complex pipeline that includes plant prediction (Wang et al., 2022).

We evaluated performance by using Dice loss and the Intersection over Union (IoU) score in the segmentation phase. Dice loss measures the similarity between the predicted segmentation and the ground truth, complemented by the IoU score, which measures the overlap between the predicted and actual segmentation areas. This dual-metric approach enabled a comprehensive assessment of the model's segmentation accuracy. Our training data set achieved exemplary performance: Dice loss

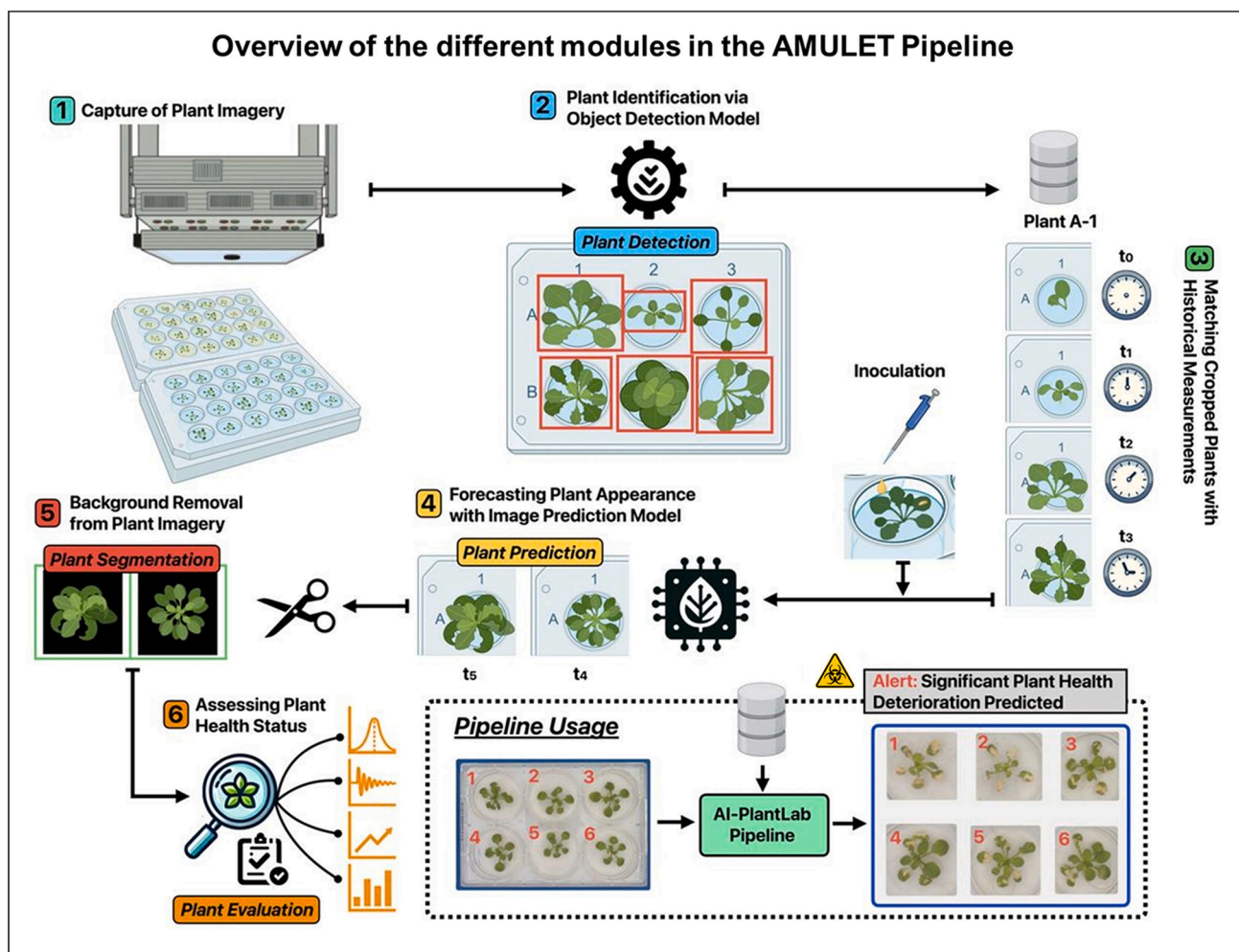


Fig. 2. The illustration presents the six stages of the AMULET workflow: (1) Capture of Plant Imagery: High-resolution RGB images of *Arabidopsis thaliana* plants are obtained. (2) Plant Identification via Object Detection Model: Plants are localised and framed within the images. (3) Matching Cropped Plants with Historical Measurements: Cropped plants are paired with historical data, creating a time series. (4) Forecasting Plant Appearance with Image Prediction Model: Future plant growth is predicted based on historical images. (5) Background Removal from Plant Imagery: Segmentation isolates the plant rosette from the background. (6) Assessing Plant Health Status: Plant health is evaluated using a model trained on morphological, physiological, and colour descriptors. The pipeline usage is showcased in the bottom right of the image, depicting the input image and the resulting predictions.

of 0.0104 alongside an IoU score of 0.9948. Moreover, the evaluation of the validation set revealed a Dice loss of 0.0135 and an IoU score of 0.9932, and analysis of the test set showed a Dice loss of 0.0127 and an IoU score of 0.9936. Such results underscore the model's robust and consistent performance, irrespective of the utilised dataset. This uniformity in high-quality performance accentuates the model's reliability in various contexts.

2.3. Statistical analysis of the plant descriptors

The final stage of our study involved a plant *evaluation* model trained to evaluate 24 distinct descriptors of plant morphology and colour changes derived from simple RGB images obtained using the Data Analyzer (PSI, Czech Republic) software in our PlantScreen™ systems. These traits were chosen due to the cost-effectiveness of RGB cameras and the heritability and reproducibility of morphological traits related to biomass, making them highly comparable between laboratory and field settings (Bouidghaghen et al., 2023). We statistically analysed these descriptors to understand the population variability of *Arabidopsis* seedlings responding to *Pst* inoculation at 24 hpi (Fig. 3). Principal Component Analysis (PCA) captured significant variability in infection progression, with the two first principal components accounting for

47.7 % of the total model variance, distinguishing between plants with larger lesions (major infection) and smaller lesions (minor infection) (Fig. 3A). This result underscored the need to increase the number of biological replicates in plant science studies to capture diversity.

A correlation analysis of the 24 descriptors revealed two distinct groups (Fig. 3B). The first group showed a positive correlation between traits like *Arabidopsis* rosette area (AREA_PX, defined as the number of green pixels), roundness, compactness, and shades of green (e.g., RGB values of 106: 113: 48 and 118: 127: 55) (Fig. 3B). The second group showed a positive correlation between lesion size (Lesion_segmentation) in *Arabidopsis* leaves at 24 h post-*Pst* inoculation and a range of colours from brown to yellow (Fig. 3B). Notably, the rosette perimeter (PERIMETER_PX) and area were uncorrelated, highlighting that the perimeter provided unique and valuable information for inclusion in the model (Fig. 3B). Perimeter and compactness have been reported to change rapidly in *Arabidopsis* plants under abiotic stress (Gao et al., 2020). Similarly, our results highlighted these parameters as promising markers for studying *Arabidopsis* responses to biotic stress, particularly *Arabidopsis-Pst*. Overall, traits like rosette area, perimeter, roundness, specific colours, and lesion size give complementary insights into the plant response to *Pst* infection.

Further evidence of population variability in *Arabidopsis* response to

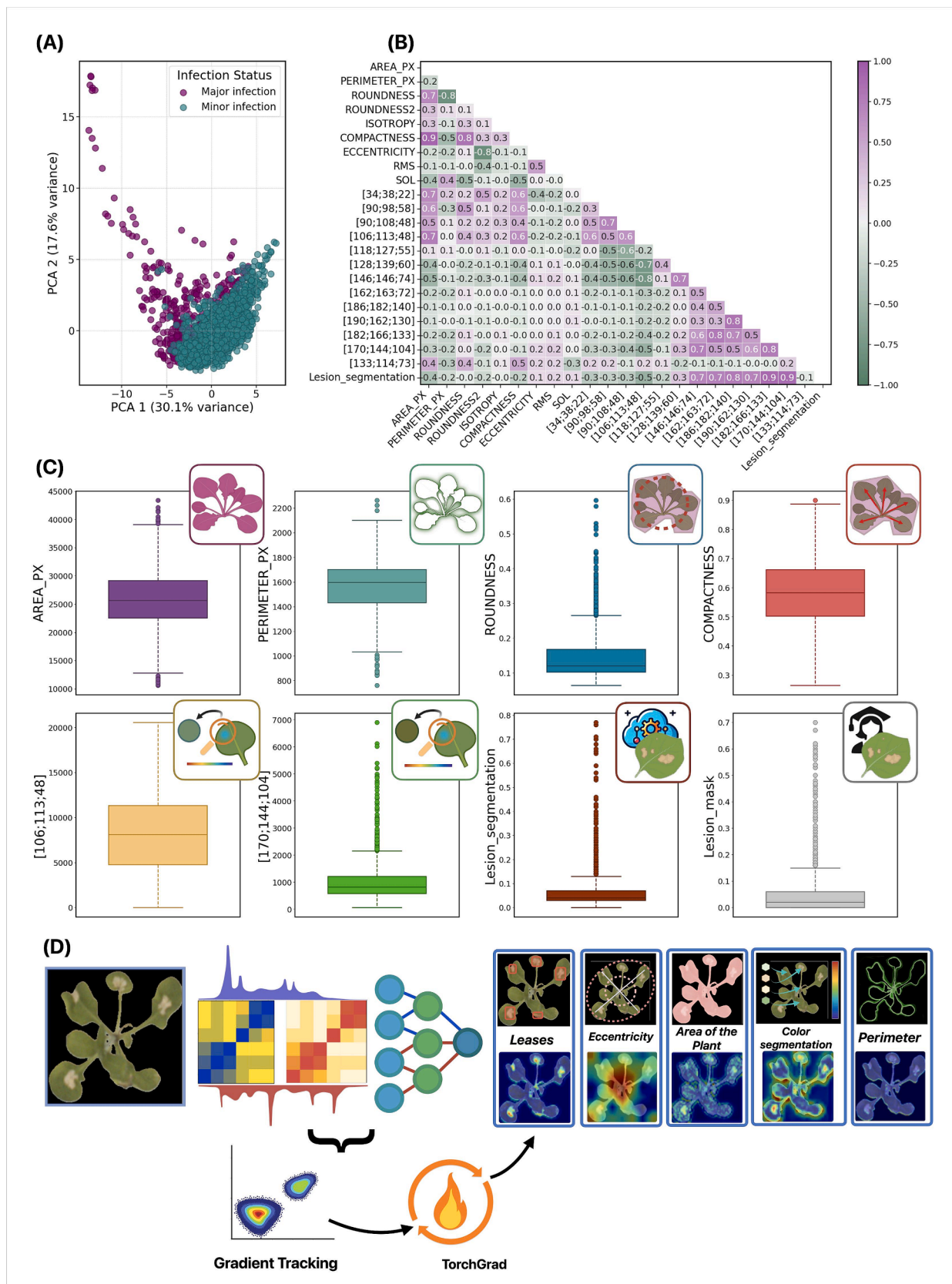


Fig. 3. Statistical analysis and TorchGrad. **(A)** Principal component analysis (PCA) representing the population variability of two-week-old *Arabidopsis thaliana* Col-0 accession plants at 24 hpi with *Pseudomonas syringae* pv. *tomato* DC3000. **(B)** Correlation matrix between the morphological and colour-related descriptors obtained from the analysis of the RGB images. **(C)** Box plot of the most interesting descriptors. **(D)** TorchGrad highlights the most important image regions using the target gradients and their equivalence to the descriptors.

Pst inoculation was observed in the box plot representations (Fig. 3C). These visualisations showed the most varied distributions for descriptors such as area and perimeter, roundness, compactness, and specific shades of green (RGB values 106: 113: 48, and 118: 127: 55). The box plots also indicated a normal distribution of the plant changes represented by these descriptors with only a few outliers (Fig. 3C). Interestingly, strong positive correlations were found among the changes in the data obtained from several descriptors, such as area, compactness, and specific green colours (e.g., 106: 113: 48). This behaviour suggests a complex interaction between plant morphological parameters and colour traits in response to pathogen exposure.

Given the representativeness of the selected descriptors in our experimental setup, we used them in our plant *evaluation* models, which included more than 2,000 manually labelled plants. We fine-tuned various models for descriptor estimation, replacing the last classification layer with a regression layer. Using Microsoft ResNet50 as the teacher model and GhostNet v2 as the student model, we achieved high performance (R^2 score of 0.9289), demonstrating the effectiveness of knowledge distillation in transferring robust feature detection capabilities to a more computationally efficient model. To ensure the robustness and efficiency of our pipeline, we employed Explainable AI (XAI) techniques, including TorchGrad and Gradient-weighted Class Activation Mapping (Grad-CAM). This technique highlighted important image regions using the target gradients to confirm that the plant evaluation model accurately focuses on relevant descriptors (Fig. 3D). The comparison between Grad-CAM outputs and the selected descriptors confirmed that our ML model could effectively integrate the pertinent descriptors defining the Arabidopsis response to *Pst* inoculation. Moreover, these techniques also allow the identification of new descriptors related to plant growth and health status hidden in the latent *phenom*, such as eccentricity or compactness. This approach also facilitated a detailed evaluation of the model's ability to identify and classify infected plants accurately, underscoring the potential of AMULET for rapid adaptation to different plant species and growth conditions (Karim et al., 2024; Shukla et al., 2020).

2.4. AMULET validation. A case study using *in vitro* potato plants

Although AMULET was initially developed using Arabidopsis for training and testing, the pipeline is specifically designed for rapid adaptation to other plant species. The pre-trained models within the pipeline serve as robust backbones readily applicable across various contexts, from plant identification to evaluation. While these models offer a strong starting point, they typically require minor fine-tuning on small species-specific datasets to achieve optimal performances. This flexibility makes AMULET a highly versatile tool for agricultural applications, enabling a smooth transition between different species with minimal adjustments.

To demonstrate the versatility of AMULET, we adapted the plant *detection* and *prediction* tasks to analyse the growth of *in vitro* potato plants. *In vitro* techniques are crucial in potato research because they are the most commonly used methods for conserving global varieties in gene banks (Bamberg et al., 2016) (https://cipotato.org/genebankcip/process/active_collection/). These techniques allow for easy, space-efficient propagation and maintenance of many plant species, from annuals to perennials (FAO, 2014) (<https://www.genebanks.org/the-platform/conservation-module/in-vitro/>). With this aim, we developed a straightforward *in vitro* protocol for phenotyping potato plants using an affordable in-house small phenotyper equipped with Raspberry Pi Zero paired with a Raspberry Pi Camera V2 and LED lights for homogeneous illumination of the plants during image capture (Supplementary Fig. S4). *In vitro* potato plants were grown in square assay tubes, with covers allowing gas exchange for more natural growth and avoiding condensation (Supplementary Fig. S4). Potato plant development initiates from a single explant segment with a unique axillary bud, growing vertically into a new shoot with clear apical

dominance. The explants were imaged vertically using a side-view RGB camera, presenting significant differences from our previous datasets (Fig. 4A). Automating plant *detection* and *predicting* explant development under varying conditions can expedite the selection of optimal protocols. Moreover, integrating these techniques into the protocol for *in vitro* potato growth (or other relevant plant species conserved using *in vitro* approaches, including trees) facilitates the development of ultra-rapid screening methods to study potato resistance to different stressors using HTP screening.

Our study used approximately 100 pictures of potato plants grown *in vitro* over 15 days. We leveraged the pre-trained backbones from the plant detection and prediction phases. Figure (4B1) illustrates the initial detection performance of the *in vitro* potato plants capable of recognising individual plants. Although some mistakes were encountered, such as misidentifying separated parts of a plant or truncating the plant image, we addressed these issues by fine-tuning the pre-trained model on a smaller, targeted dataset of potato plants (100 annotated images for training and 40 for validation), allowing it to adjust parameters for improved accuracy (Fig. 4B2). Leveraging the generalisation capability from extensive initial training, the model requires only a limited dataset, making the fine-tuning process efficient and effective, with solid performance gains achieved in minimal training time (hours).

Similarly, as illustrated in Fig. 4B3, the image *prediction* phase for *in vitro* potato plants was fine-tuned. The blue section represents ground truth data from time steps T_1 to T_9 , while the red section displays the predictions made by the fine-tuned model. Fig. 4B4 presents a comparison of several error metrics, namely Mean Squared Error (MSE), Mean Absolute Error (MAE), 1/Peak Signal-to-Noise Ratio (1/PSNR), and Normalised Root Mean Squared Error (NRMSE), quantifying the difference between the predicted plant images and the corresponding ground truths at each time-step. These metrics highlight the effectiveness of fine-tuning the pre-trained AMULET module in improving prediction capabilities. Moreover, our pipeline has proven adaptable to various plant species and growth conditions, providing a well-developed starting point for rapid fine-tuning. Moreover, the comprehensive nature of AMULET includes all necessary steps for processing plant phenotyping data, from detection to evaluation, streamlining the workflow, and saving valuable time once the imaging process concludes.

3. Conclusion

AMULET is a modular and efficient solution for a fast image processing obtained from non-invasive phenotyping using an affordable RGB camera. It enhances phenotyping by offering prediction, empowering SimVP as an ML model with high prediction capabilities. This skill will benefit stakeholders, ranging from the plant science community to crop growers, by shortening experiment timelines, and by an earlier stress detection, and quicker identification of unhealthy plants, enabling faster treatment and better crop management.

Beyond traditional phenotyping, AMULET enables the exploration of the *latent phenom*—hidden patterns and traits that might not be immediately visible to human observation, via TorchGrad and Gradient-weighted Class Activation Mapping. Leveraging AI, AMULET is able to identify emergent phenotypic signatures that could be biologically significant but previously overlooked, extending its capability beyond detecting predefined characteristics.

Trained on a large image dataset of Arabidopsis seedlings at various developmental stages, including tiny 3-day-old seedlings (2–4 mm diameter), AMULET has demonstrated remarkable adaptability to other plant species. For instance, it was successfully fine-tuned for *in vitro* potato plants, overcoming challenges related to their different growth habits. This adjustment required only a minimal dataset and significantly less time and resource than building a model from scratch. Originally trained using high-resolution data from the PlantScreenTM XYZ that use an expensive, high-resolution RGB camera, AMULET's pre-trained ML backbone can be effectively used with more accessible, low-

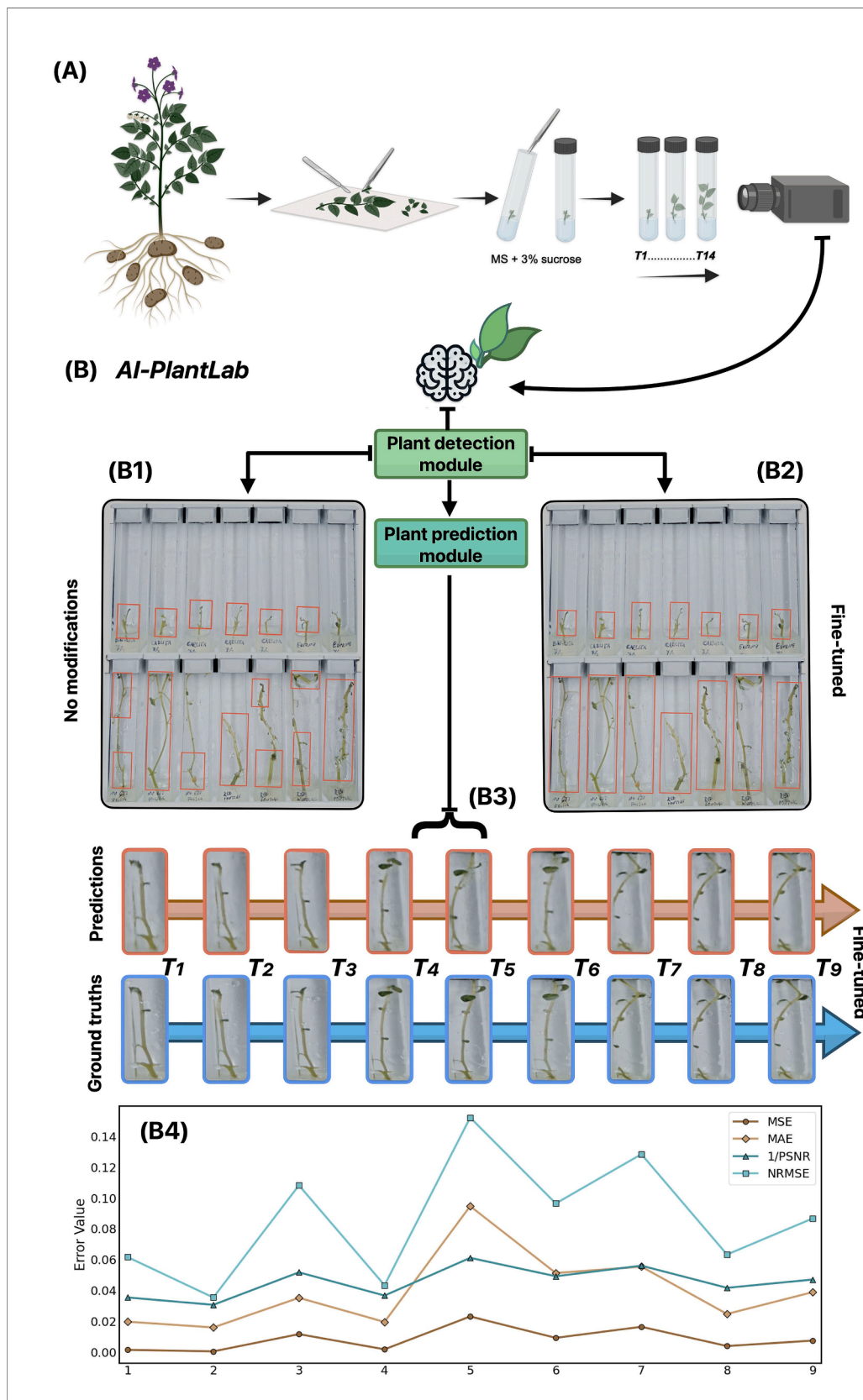


Fig. 4. AMULET validation using *in vitro* potato plants. Adaptation of the AMULET pipeline to *in vitro* potato plants. Created in BioRender. De Diego, N. (2025) <https://BioRender.com/h82q650> (A) A new protocol for *in vitro* potato imaging using side-view RGB camera. (B1) Plant detection using the pre-trained model without modifications. (B2) Improved plant detection after fine-tuning the model. (B3) Fine-tuned image predictions for *in vitro* potato plants: the blue section represents ground truth data from time steps T1 to T9, and the red section illustrates the prediction made by the fine-tuned model. (B4) Error metrics (MSE, MAE, 1/PSNR, NRMSE) for the predicted and ground truth images at each time step showcasing the impact of fine-tuning on the pre-trained AMULET modules. (For interpretation of the references to colour in this figure legend, the reader is referred to the web version of this article.)

cost RGB cameras (**Supplementary Fig. S4**), making advanced phenotyping widely attainable.

AMULET has also proven effective in predicting disease onset in *Arabidopsis* seedlings hours before visible symptoms appear, offering potential for early interventions to minimise productivity losses. It can predict growth patterns for different growth habits, like *Arabidopsis* and potatoes, aiding in optimising protocols needed in Gene Banks, potentially accelerating the conservation and maintenance of a wide range of plant species, including recalcitrant ones.

The success of AMULET needs to be further challenged with infinite combinations of environmental conditions and plant species to strengthen its versatility. Nevertheless, its ability to streamline phenotyping – from detection to data analysis – positions it as a transformative and breakthrough tool in plant science. AMULET's integration into breeding programs and agricultural management could optimise crop vitality and yield, empowering researchers and growers to implement proactive strategies that ensure plant vitality and yield, reducing the effort and time needed after imaging and empowering more proactive plant care strategies.

4. Material and methods

4.1. Plant material and growth conditions

Arabidopsis thaliana ecotype Col-0 seeds were acquired from the Salk Institute Genomic Analysis Laboratory (<https://www.signal.salk.edu/cgi-bin/tdnaexpress>). Firstly, the seeds were surface sterilised and seeded on square plates (12 cm × 12 cm) containing 0.5 × Murashige and Skoog (MS) medium [55] (pH 5.7) supplemented with 0.6 % gelling agent (Phytigel, Sigma–Aldrich, Germany) and maintained for three days at 4 °C in the dark (De Diego et al., 2017). Afterwards, the plates were transferred to a growth chamber with controlled conditions (22 °C, 16/8h light/dark cycle, a light intensity of 120 μmol photons of PAR m⁻² s⁻¹) and placed vertically. Four days later, seedlings of similar size were transferred under sterile conditions to 6-, 12- and 24-well plates with one seedling per well, and the plates were sealed with perforated transparent foil, allowing gas and water exchange. Each well contained different amounts of full MS medium (pH 5.7; supplemented with 0.6 % Phytigel), according to the plate format. The plates were transferred to the Olophen platform equipped with the PlantScreen™ XYZ (De Diego et al., 2017) or Compact system (Marchetti et al., 2019). *Arabidopsis* seedlings were grown for a period ranging from seven to fourteen days, varying based on the number of wells in the plates, under controlled conditions (22/20 °C, 16/8h light/dark cycle, a light intensity of 120 μmol photons of PAR m⁻² s⁻¹, 60 % relative humidity) on the Olophen platform.

We used six different potato varieties (Agria, Baraka, Carlita, Kennebec, Nu 633 Frisia, and Red Pontiac) multiplied *in vitro* for the case study. The material was obtained from healthy, disease-free mother plants grown *in vitro* and provided by NEIKER (Vitoria-Gasteiz, Spain). 7–10 mm mono-nodal segments containing one axillar bud each were cut from the mother plants, and leaves were excised. The nodes were then transferred to 7.7 × 7.7 × 9.7 cm magenta boxes (Sigma-Aldrich, Darmstadt, Germany) filled with 75 mL of full MS media, supplemented with 30 g/L sucrose, 8 g/L agar, pH = 5.7). Between 9 and 12 nodes were transferred into the magenta box to keep the plant material. Explants were kept in a Conviron CMP 6010 growth chamber (Conviron, Winnipeg, Canada) at 22 °C, under a light intensity of 80 μmol photons m⁻² s⁻¹, in long-day photoperiod (16 h day / 8 h night), until they had generated enough internodes (4–5 weeks) for multiplying the explants to start the non-invasive phenotyping.

Plastic tubes (1.35 × 1.35 × 8.6 cm) (Tintometer GmbH, Dortmund, Germany) were filled with 4.3 mL of the same full MS described above for plant phenotyping. The air-tight caps were drilled four times each with a 2.5 mm bore to allow gas exchange. Each plant was subdivided into a 7–10 mm-long mono-nodal section containing one leaf and axillar

bud. The two most basal and apical nodes were discarded. The leaves of the remaining nodes were excised, and one node was carefully inserted in the centre of each phenotyping tube until approximately a third of the node remained submerged in the media. The tubes were then closed with the perforated caps, and the gap on the top of each cap was filled with autoclaved glass wool (VWR International s. r. o., Stříbrná Skalice, Czechia) to minimise contamination. The tubes were kept for four weeks in the growth chamber under the same conditions described above and photographed once per day using a Raspberry Pi Camera V2 and two stripes of cool-white LED lights for homogenous illumination. For imaging, the tubes were placed in custom 3D-printed holders, designed with a curvature that allows the clear side of each tube to align perpendicular to the RGB camera (**Supplementary Fig. S3B, C**), thus minimising the plant area that gets occluded by the edge of the tube. These holders fit into the slot of a custom 3D-printed stand (**Supplementary Fig. S3B, C**), which can be placed in a fixed position in the phenotyper (**Supplementary Fig. S3D**). This system allows for obtaining homogeneous pictures in terms of lighting and distance from the camera.

4.2. Infection assay

Two-week-old *Arabidopsis* seedlings grown in 6 well-plates were used for the infection study. Some of the seedlings were inoculated with *Pseudomonas syringae* pv. *tomato* DC3000 (*Pst*) strain as described by Jasso-Robles et al. (2020), while the rest served as controls (non-inoculated plants). The bacterium was cultured in King's B (KB) medium (King et al., 1954) supplemented with 50 μg/mL rifampicin for 24 h at 28 °C. *Pst* was resuspended in 10 mM MgCl₂ (pH 7.0) and adjusted to an OD₆₀₀ of 0.2. Five μL of the bacterial suspension were inoculated on the true leaves of *Arabidopsis* seedlings. 5 μL of MgCl₂ buffer was also applied to the remaining half of the *Arabidopsis* seedlings as a control.

4.3. Dataset characteristics and Volume

All *Arabidopsis* images were captured using high-resolution RGB cameras integrated into our PlantScreen™ XYZ or Compact system (Olophen Platform). For the initial phase of model training (plant detection), images of *Arabidopsis* seedlings grown in 6 to 24 well-plates at various developmental stages were used. The acquired images were initially annotated to identify key features, followed by extracting multiple descriptors, including morphological parameters such as the area (AREA_PX) and perimeter (PERIMETER_PX) calculated from binary images by counting pixels within the rosette and along its edge, respectively. Metrics like the relative growth rate, absolute growth rate, and colour-related indices (Green Leaf Index – GLI, Normalised Green-Red Difference Index – NGRDI, and Visible Atmospherically Resistant Index – VARI) were also calculated for each RGB image, as described by Ugena et al. (Ugena et al., 2018). These descriptors, encompassing morphological traits and colour segmentation, were meticulously correlated with their respective images to facilitate accurate plant detection and analysis. 32,526 plants were used for the plant detection task (**Supplementary Table S1**).

For the *predictive* model task, a novel dataset comprising images of *Arabidopsis* seedlings grown in 6-well plates. Two-week-old plants inoculated with *Pst* or MgCl₂ as a control were photographed at pre-determined intervals before and after inoculation (t_0 to t_5 ; 0, 3, 6, 9, 12, and 24 h) using a high-resolution RGB camera installed in our PlantScreen™ Compact system to cover a comprehensive range of conditions encompassing infected and healthy plants.

Expert verification was conducted on a separate test dataset, focusing on the morphology and health status of *Arabidopsis thaliana* (3,312 plants) to validate the predictive accuracy of the models (**Supplementary Table S1**). In this case, two additional features related to the size of the leaf lesions were also included for higher accuracy.

For the *segmentation* task, an additional 3,306 plants were carefully

selected and manually segmented to capture the diversity related to the issue, comprising 2,298 infected and 1,008 non-infected Arabidopsis seedlings (Supplementary Table S1). An additional 546 infected and 545 non-infected plants segmented by our model were also added to this dataset, and each image underwent rigorous verification to ensure relevance and accuracy.

Finally, for the plant *evaluation* task, a new dataset of 2,298 *Pst*-infected plants was chosen explicitly for annotation and further analysis (Supplementary Table S1). This dataset included additional morphological descriptors such as roundness, roundness2, and isotropy, which describe plant circularity and eccentricity, and RMS, which indicate symmetry (Pavicic et al., 2017). Parameters like compactness and SOL, which depend on the distance of the edge to the centre, were also used. Furthermore, automated (Lesion segmentation) and manual (Lesion_Mask) segmentation of each plant lesion area was included in the annotated descriptors for this phase for a more complex description of the plant health status.

4.4. AMULET details

With proper data preprocessing, partitioning, and augmentations (see Subsection- 4.5. Preprocessing and Augmentation), we utilised the initial RGB imagery of shape ($N \times 3 \times 1920 \times 2560$), where N is the number of gathered images to train the Faster Region-based Convolutional Neural Network (Faster-RCNN) for the plant *detection* task. The Faster-RCNN model, as depicted in Supplementary Fig. S1, integrates two key components: a region proposal network (RPN) for generating region proposals and a deep convolutional neural network (CNN) for the classification and bounding box refinement of these proposals. The RPN directly utilises the feature maps obtained from the input images to predict object bounds and objectness scores at each position. The CNN then processes these proposals, classifying the objects within the proposed regions and refining their locations. During the training and testing process, the Box Regression, Classification, Objectness, and RPN Box Regression losses-scores were monitored and logged to ensure the robustness of the training process for exact loss values and other parameters obtained in the training of the pipeline (Supplementary Table S1).

For the pivotal task of plant *prediction*, which takes as input image time series of shape ($N \times T \times 3 \times 224 \times 224$), where T is the number of plant images from previous measurements, we selected the Simpler yet Better Video Prediction model (SimVP). The SimVP framework utilises a CNN-based approach comprising an Encoder, Translator, and Decoder. The Encoder extracts spatial features through N_s , Conv, Norm, and ReLU blocks, operating on C channels across dimensions (H, W). The Translator captures temporal dynamics using N_t Inception modules, convolving $T \times C$ channels over (H, W). The Decoder reconstructs the future frames with N_s unConv Norm ReLU blocks, targeting C channels on (H, W). The simplified global structure of the model is available in Supplementary Fig. S1.

For the training of the plant *segmentation* step, which adopts input data of shape ($N \times 3 \times 224 \times 224$), the architecture of DeepLabV3 + was chosen integrated with the EfficientNet-B7 encoder. The simplified architecture of the DeepLabV3 + is depicted in Supplementary Fig. S1. It integrates multi-scale contextual information through atrous convolution applied at various scales within the encoder module, facilitated by the EfficientNet-B7 advanced feature extraction capabilities. To highlight the effectiveness of this trained model, plant images were segmented using a conventional segmentation system, providing a baseline for comparison and displaying images segmented by our finetuned DeepLabV3 + model. See Supplementary Table S2 for the obtained loss summary for each step.

For the final phase of the AMULET pipeline, we trained a plant *evaluation* model that takes as input segmented images ($N \times 3 \times 224 \times 224$) and their corresponding targets in the form of 24 unique descriptors ($N \times 24$). To estimate these crucial descriptors from images, we

separately trained a set of models, namely Vision Transformer (ViT) (Dosovitskiy et al., 2020), CoAtNet (Dai et al., 2021), ResNet50, and GhostNet (Tang et al., 2022), from which the best performance was exhibited by the ResNet50 (Supplementary Table S2). Furthermore, we employed knowledge distillation between combinations of the models mentioned, which resulted in the best combination of ResNet50 as the teacher and GhostNet v2 as the student, significantly outperforming other variations (Supplementary Fig. S1 and Table S2). Distillation knowledge is transferred from ResNet50 to GhostNetV2-160, utilising true and soft labels to guide the student model in replicating the teacher's analytical prowess. This approach ensures that the student model achieves comparable accuracy in terms of computational efficiency. Validating outputs from the previous tasks is quite straightforward; however, in this case, the model outputs just a list of values guided by the R^2 score.

4.5. Preprocessing and augmentation

Data preprocessing is essential for preparing raw images and auxiliary inputs, significantly impacting algorithm performance in training and deployment. This is particularly important for complex data like the Arabidopsis dataset. The normalisation preprocessing step was applied for plant *detection*, *prediction*, *segmentation*, and *evaluation*, ensuring a uniform range for pixel values. Additionally, we standardise descriptors extracted from segmented images, which serve as target labels in the Plant Evaluation step, to ensure balanced contributions to the model's learning process. Furthermore, a plant position validation procedure assigning a unique identifier to each plant following a systematic convention was created as detailed in Supplementary material- Algorithm 1 and illustrated in Supplementary Fig. S1. This identification begins with the plant located at the top-left and progresses horizontally across the image.

Moreover, dynamic thresholding accommodated plant growth between consecutive time points. This method involves evaluating the plant size bounding box in sequential images and making necessary adjustments based on a predefined growth rate threshold. Supplementary material- Algorithm 1 details the procedural steps for detecting, organising, and assigning unique indices to plants within a given image. These steps adhere to a systematic workflow that includes loading the image, applying a pre-trained model, extracting and sorting detected plants, and assigning positions based on a vertical threshold and row-wise organisation. Additionally, Supplementary Fig. S2 demonstrates its practical application. The centring equation inside Supplementary material- Algorithm 1 that calculates the centre of the bounding box is defined as follows:

$$Center = \left(\frac{x_{min} + x_{max}}{2}, \frac{y_{min} + y_{max}}{2} \right) \quad (1)$$

where x_{min} and x_{max} represent the minimum and maximum x-coordinate values of the bounding box, determining the leftmost and rightmost boundaries of the object detected in the image, respectively. Similarly, y_{min} and y_{max} denote the minimum and maximum y-coordinate values of the bounding box, defining the bottom and top boundaries of the object, respectively (see Supplementary Fig. S2 and Supplementary material- Algorithm 1).

Additionally, we examined the plant changes and development and excluded Arabidopsis plants with no or minimal growth in subsequent images from the dataset. This systematic approach ensures that our models remain sensitive to the natural variability in plant sizes and maintain the integrity of temporal data analysis.

Despite generating high-quality data, data augmentation remains essential for training models. Introducing diverse variations through augmentation significantly enriches the dataset, enhancing model performance. Augmentation strategies are applied at each pipeline stage, ensuring comprehensive enhancement of the dataset diversity. Several

augmentations were used throughout the pipeline, such as brightness adjustments to simulate diurnal variations in sunlight exposure at different times of the day. Gaussian blur was applied to emulate the blurring effects that might occur during data collection, introducing the model to potential variances in image clarity.

Additionally, random positioning augmentation ensures geometric variability of plant placements within images, enriching the dataset with a broader range of positional contexts. Rotation augmentations were introduced at certain pipeline stages to account for orientation variability. For a summary of augmentations used in each step of the training pipeline, see [Supplementary Table S3](#).

CRedit authorship contribution statement

Jan Zdrzil: Writing – review & editing, Writing – original draft, Visualization, Validation, Software, Methodology, Investigation, Formal analysis, Data curation, Conceptualization. **Lingping Kong:** Writing – original draft, Software, Methodology, Investigation, Formal analysis. **Pavel Klimeš:** Methodology, Investigation, Data curation. **Francisco Ignacio Jasso-Robles:** Methodology, Investigation, Formal analysis. **Iñigo Saiz-Fernández:** Methodology, Investigation, Data curation. **Firat Güder:** Writing – review & editing, Supervision, Methodology, Investigation. **Lukáš Spíchal:** Writing – review & editing, Supervision, Methodology, Investigation, Conceptualization. **Václav Snášel:** Writing – review & editing, Supervision, Software, Resources, Investigation, Funding acquisition. **Nuria De Diego:** Writing – review & editing, Writing – original draft, Visualization, Validation, Supervision, Resources, Methodology, Investigation, Funding acquisition, Formal analysis, Data curation, Conceptualization.

Declaration of Generative AI and AI-assisted technologies in the writing process

While preparing this work, the author(s) used ChatGPT and Grammarly to improve language and readability and ChatGPT to design concrete icons integrated into the figures. After using this tool/service, we reviewed and edited the content as needed, and we take full responsibility for the publication's content.

Funding

This publication was funded by the project PATAFEST funded by the European Union under the grant number 101084284. The views and opinions expressed are solely those of the author(s) and do not necessarily reflect those of the European Union or the European Research Executive Agency (REA). Neither the European Union nor the granting authority can be held responsible for them. This publication was also funded by the project JG_2024_036, implemented within the Palacky University Young Researcher Grant and SP2024/007 Zpracování a pokročilá analýza biomedicínských dat IX.

Declaration of competing interest

The authors declare that they have no known competing financial interests or personal relationships that could have appeared to influence the work reported in this paper.

Acknowledgements

We thank Jana Nosková and Andrea Hybenová for their technical support. We thank NEIKER, particularly Dr. Jose Ignacio Ruiz de Galarreta and Dr. Amaia Ortiz-Barredo, for providing the *in vitro* potato material. Graphical abstract was created in BioRender, De Diego, N. (2025), <https://BioRender.com/a28v264>. F.G. thanks the Bill and Melinda Gates Foundation (INV-038695) and Bezos Earth Fund through the Bezos Centre for Sustainable Protein (BCSP/IC/001).

Author contribution

J.Z., F.G., L.S., V.S., and N.D.D. conceived the manuscript's structure. J.Z and N.D.D. led the writing of the manuscript and experimental work. P.K., F.I.J.-R. and I.S.-F. contributed to experimental work regarding plant phenotyping. J.Z and L.K. contributed to the experimental work regarding machine learning models. J.Z., L.K., P.K., F.G., L.S., V.S., and N.D.D. contributed to the writing of the manuscript. All authors reviewed and agreed on the manuscript before submission.

Appendix A. Supplementary data

Supplementary data to this article can be found online at <https://doi.org/10.1016/j.compag.2025.110390>.

Data availability

Data will be made available on request.

References

- Anshori, M.F., Dirpan, A., Sitaesmi, T., Rossi, R., Farid, M., Hairmansis, A., Purwoko, B., Suwarno, W.B., Nugraha, Y., 2023. An overview of image-based phenotyping as an adaptive 4.0 technology for studying plant abiotic stress: a bibliometric and literature review. *Heliyon* 9, e21650. <https://doi.org/10.1016/j.heliyon.2023.e21650>.
- Aytekin, B., Mardani-Aghabaglou, A., 2022. Sustainable materials: a review of recycled concrete aggregate utilisation as pavement material. *Transportation Research Record: Journal of the Transportation Research Board* 2676, 468–491. <https://doi.org/10.1177/03611981211052026>.
- Bamberg, J.B., Martin, M.W., Abad, J., Jenderek, M.M., Tanner, J., Donnelly, D.J., Nassar, A.M.K., Veilleux, R.E., Novy, R.G., 2016. *In vitro* technology at the US potato genebank. *In Vitro Cellular & Developmental Biology - Plant* 52, 213–225. <https://doi.org/10.1007/s11627-016-9753-x>.
- Bhugra, S., Srivastava, S., Kaushik, V., Mukherjee, P., Lall, B., 2024. Plant data generation with generative AI: an application to plant phenotyping. In: *Applications of Generative AI*. Springer International Publishing, Cham, pp. 503–535. [10.1007/978-3-031-46238-2_26](https://doi.org/10.1007/978-3-031-46238-2_26).
- Bouidghaghen, J., Moreau, L., Beauchêne, K., Chapuis, R., Mangel, N., Cabrera-Bosquet, L., Welcker, C., Bogard, M., Tardieu, F., 2023. Robotised indoor phenotyping allows genomic prediction of adaptive traits in the field. *Nat Commun* 14, 6603. <https://doi.org/10.1038/s41467-023-42298-z>.
- Bryksová, M., Hybenová, A., Hernández, A.E., Novák, O., Pěncík, A., Spíchal, L., De Diego, N., Doležal, K., 2020. Hormopriming to mitigate abiotic stress effects: a case study of N^2 -substituted cytokinin derivatives with a fluorinated carbohydrate moiety. *Front Plant Sci* 11, 599228. <https://doi.org/10.3389/fpls.2020.599228>.
- Chen, L.-C., Zhu, Y., Papandreou, G., Schroff, F., Adam, H., 2018. Encoder-decoder with atrous separable convolution for semantic image segmentation. *ArXiv*.
- Chitwood, D.H., Topp, C.N., 2015. Revealing plant cryptotypes: defining meaningful phenotypes among infinite traits. *Curr Opin Plant Biol* 24, 54–60. <https://doi.org/10.1016/j.pbi.2015.01.009>.
- Dai, Z., Liu, H., Le, Q.V., Tan, M., 2021. CoAtNet: marrying convolution and attention for all data sizes. *ArXiv*.
- De Diego, N., Fürst, T., Humplík, J.F., Ugena, L., Podlešáková, K., Spíchal, L., 2017. An automated method for high-throughput screening of Arabidopsis rosette growth in multi-well plates and its validation in stress conditions. *Front Plant Sci* 8, 1702. <https://doi.org/10.3389/fpls.2017.01702>.
- Dosovitskiy, A., Beyer, L., Kolesnikov, A., Weissenborn, D., Zhai, X., Unterthiner, T., Dehghani, M., Minderer, M., Heigold, G., Gelly, S., Uszkoreit, J., Houslsby, N., 2020. An image is worth 16x16 words: transformers for image recognition at scale. *ArXiv*.
- FAO, 2014. Genebank standards for plant genetic resources for food and agriculture.
- Fiorani, F., Schurr, U., 2013. Future scenarios for plant phenotyping. *Annu Rev Plant Biol* 64, 267–291. <https://doi.org/10.1146/annurev-arplant-050312-120137>.
- Gao, G., Tester, M.A., Julkowska, M.M., 2020. The use of high-throughput phenotyping for assessment of heat stress-induced changes in Arabidopsis. *Plant Phenomics* 2020. <https://doi.org/10.34133/2020/3723916>.
- Gao, Z., Tan, C., Wu, L., Li, S.Z., 2022. SimVP: Simpler yet better Video Prediction. *ArXiv* 2206.05099.
- Gibbs, J.A., Burgess, A.J., 2024. Application of deep learning for the analysis of stomata: a review of current methods and future directions. *J Exp Bot* 75 (21), 6704–6718. <https://doi.org/10.1093/jxb/erae207>.
- Han, D., Choo, M., Im, J., Shin, Y., Lee, J., Jung, S., 2023. Precipitation nowcasting using ground radar data and simpler yet better video prediction deep learning. *Gisci Remote Sens* 60 (1). <https://doi.org/10.1080/15481603.2023.2203363>.
- Harfouche, A.L., Nakhle, F., Harfouche, A.H., Sardella, O.G., Dart, E., Jacobson, D., 2023. A primer on artificial intelligence in plant digital phenomics: embarking on the data to insights journey. *Trends Plant Sci* 28, 154–184. <https://doi.org/10.1016/j.tplants.2022.08.021>.

- Harkat, H., Nascimento, J., Bernardino, A., 2020. Fire segmentation using a DeepLabv3+ architecture. In: Bruzzone, L., Bovolo, F., Santi, E. (Eds.), *Image and Signal Processing for Remote Sensing XXVI*. Bellingham.
- Isak, M.A., Bozkurt, T., Tütüncü, M., Dönmez, D., İzgü, T., Şimşek, Ö., 2024. Leveraging machine learning to unravel the impact of cadmium stress on goji berry micropropagation. *PLoS One* 19, e0305111. <https://doi.org/10.1371/journal.pone.0305111>.
- Jasso-Robles, F.I., Aucique-Perez, C.E., Zeljković, S.Č., Saiz-Fernández, I., Klimeš, P., De Diego, N., 2024. The loss-of-function of *AtNATA2* enhances *AtADC2*-dependent putrescine biosynthesis and priming, improving growth and salinity tolerance in *Arabidopsis*. *Physiol Plant* 176 (6), e14603. <https://doi.org/10.1111/ppl.14603>.
- Jasso-Robles, F.I., Gonzalez, M.E., Pieckenstein, F.L., Ramírez-García, J.M., de la Guerrero-González, M.de.la.L., Jiménez-Bremont, J.F., Rodríguez-Kessler, M., 2020. Decrease of *Arabidopsis* PAO activity entails increased RBOH activity, ROS content and altered responses to *Pseudomonas*. *Plant Sci.* 292, 110372. <https://doi.org/10.1016/j.plantsci.2019.110372>.
- Kapoor, S., Cantrell, E.M., Peng, K., Pham, T.H., Bail, C.A., Gundersen, O.E., Hofman, J. M., Hullman, J., Lones, M.A., Malik, M.M., Nanayakkara, P., Poldrack, R.A., Raji, I. D., Roberts, M., Salganik, M.J., Serra-Garcia, M., Stewart, B.M., Vandewiele, G., Narayanan, A., 2024. REFORMS: consensus-based REcommendations FOR MACHIne-learning-based science. *Sci Adv* 10 (18). <https://doi.org/10.1126/sciadv.adk3452>.
- Karim, M.J., Goni, M.O.F., Nahiduzzaman, Md., Ahsan, M., Haider, J., Kowalski, M., 2024. Enhancing agriculture through real-time grape leaf disease classification via an edge device with a lightweight CNN architecture and Grad-CAM. *Sci Rep* 14, 16022. <https://doi.org/10.1038/s41598-024-66989-9>.
- King, E.O., Ward, M.K., Raney, D.E., 1954. Two simple media for the demonstration of pyocyanin and fluorescin. *J Lab Clin Med* 44, 301–307.
- Koornneef, M., Meinke, D., 2010. The development of *Arabidopsis* as a model plant. *Plant J.* 61, 909–921. <https://doi.org/10.1111/j.1365-313X.2009.04086.x>.
- Kovach, M., McCouch, S., 2008. Leveraging natural diversity: back through the bottleneck. *Curr Opin Plant Biol* 11, 193–200. <https://doi.org/10.1016/j.pbi.2007.12.006>.
- Lee, S.-J., Lee, Y., 2024. PredRNNv2-based drought prediction using Vegetation Health Index (VHI). in: EGU General Assembly Conference Abstracts. p. 14437. doi: 10.5194/egusphere-egu24-14437.
- Li, K., Zhang, L., Li, B., Li, S., Ma, J., 2022. Attention-optimised DeepLab V3 + for automatic estimation of cucumber disease severity. *Plant Methods* 18, 109. <https://doi.org/10.1186/s13007-022-00941-8>.
- Li, M., Liao, Y., Lu, Z., Sun, M., Lai, H., 2023. Non-destructive monitoring method for leaf area of *Brassica napus* based on image processing and deep learning. *Front Plant Sci* 14, 1163700. <https://doi.org/10.3389/fpls.2023.1163700>.
- Lippmann, R., Babben, S., Menger, A., Delker, C., Quint, M., 2019. Development of wild and cultivated plants under global warming conditions. *Curr. Biol.* 29, R1326–R1338. <https://doi.org/10.1016/j.cub.2019.10.016>.
- Mahmood, M.A., Alsalem, K., 2024. Olive leaf disease detection via wavelet transform and feature fusion of pre-trained deep learning models. *Computers, Materials & Continua* 78, 3431–3448. <https://doi.org/10.32604/cmc.2024.047604>.
- Marchetti, C.F., Ugena, L., Humpfík, J.F., Polák, M., Čávar Zeljković, S., Podlešáková, K., Fürst, T., De Diego, N., Spíchal, L., 2019. A novel image-based screening method to study water-deficit response and recovery of barley populations using canopy dynamics phenotyping and simple metabolite profiling. *Front Plant Sci.* 10, 1252. <https://doi.org/10.3389/fpls.2019.01252>.
- Mertens, S., Verbraeken, L., Sprenger, H., De Meyer, S., Demuynck, K., Cannoot, B., Merchie, J., De Block, J., Vogel, J.T., Bruce, W., Nelissen, H., Maere, S., Inzé, D., Wuyts, N., 2023. Monitoring of drought stress and transpiration rate using proximal thermal and hyperspectral imaging in an indoor automated plant phenotyping platform. *Plant Methods* 19, 132. <https://doi.org/10.1186/s13007-023-01102-1>.
- Pavicic, M., Mouhu, K., Wang, F., Bilička, M., Chovanček, E., Himanen, K., 2017. Genomic and phenomic screens for flower related RING type ubiquitin E3 ligases in *Arabidopsis*. *Front Plant Sci* 8, 416. <https://doi.org/10.3389/fpls.2017.00416>.
- Polly, R., Devi, E.A., 2024. Semantic segmentation for plant leaf disease classification and damage detection: a deep learning approach. *Smart Agric. Technol.* 9, 100526. <https://doi.org/10.1016/j.atech.2024.100526>.
- Ren, S., He, K., Girshick, R., Sun, J., 2017. Faster R-CNN: towards real-time object detection with region proposal networks. *IEEE Trans Pattern Anal Mach Intell* 39, 1137–1149. <https://doi.org/10.1109/TPAMI.2016.2577031>.
- Rouphael, Y., Spíchal, L., Panzarová, K., Casa, R., Colla, G., 2018. High-throughput plant phenotyping for developing novel biostimulants: from lab to field or from field to lab? *Front Plant Sci* 9, 1197. <https://doi.org/10.3389/fpls.2018.01197>.
- Sharma, T., Sethi, G.K., 2024. Improving wheat leaf disease image classification with point cloud segmentation technique. *SN Comput Sci* 5, 244. <https://doi.org/10.1007/s42979-023-02571-w>.
- Shi, X., Chen, Z., Wang, H., Yeung, D.-Y., Wong, W., Woo, W., 2015. Convolutional LSTM network: a machine learning approach for precipitation nowcasting. *arXiv* 1506.04214.
- Shoib, M., Shah, B., El-Sappagh, S., Ali, A., Ullah, A., Alenezi, F., Gechev, T., Hussain, T., Ali, F., 2023. An advanced deep learning models-based plant disease detection: a review of recent research. *Front Plant Sci* 14, 1158933. <https://doi.org/10.3389/fpls.2023.1158933>.
- Shukla, N., Palwe, S., Shubham, Rajani, M., Suri, A., 2020. Plant disease detection and localisation using GRAD-CAM. *International Journal of Recent Technology and Engineering (IJRTE)* 8, 3069–3075. <https://doi.org/10.35940/ijrte.E6935.038620>.
- Singh, A., Jones, S., Ganapathysubramanian, B., Sarkar, S., Mueller, D., Sandhu, K., Nagasubramanian, K., 2021. Challenges and opportunities in machine-augmented plant stress phenotyping. *Trends Plant Sci* 26, 53–69. <https://doi.org/10.1016/j.tplants.2020.07.010>.
- Son, D., Park, J., Lee, S., Kim, J.J., Chung, S., 2024. Integrating non-invasive VIS-NIR and biomedicine spectroscopies for stress classification of sweet basil (*Ocimum basilicum* L.) with machine learning. *Biosens Bioelectron* 263, 116579. <https://doi.org/10.1016/j.bios.2024.116579>.
- Sorrentino, M., De Diego, N., Ugena, L., Spíchal, L., Lucini, L., Miras-Moreno, B., Zhang, L., Rouphael, Y., Colla, G., Panzarová, K., 2021. Seed priming with protein hydrolysates improves *Arabidopsis* growth and stress tolerance to abiotic stresses. *Front Plant Sci* 12, 626301. <https://doi.org/10.3389/fpls.2021.626301>.
- Su, Y., Li, D., Chen, X., 2021. Lung nodule detection based on Faster R-CNN framework. *Comput Methods Programs Biomed* 200, 105866. <https://doi.org/10.1016/j.cmpb.2020.105866>.
- Tan, C., Gao, Z., Wu, L., Xu, Y., Xia, J., Li, S., Li, S.Z., 2023. Temporal Attention Unit: towards efficient spatiotemporal predictive learning. *ArXiv* 2206.12126.
- Tang, Y., Han, K., Guo, J., Xu, C., Xu, C., Wang, Y., 2022. GhostNetV2: enhance cheap operation with long-range attention. *ArXiv*.
- Townsend, T., 2020. World natural fibre production and employment. In: *Handbook of Natural Fibres*. Elsevier, pp. 15–36. <https://doi.org/10.1016/B978-0-12-818398-4.00002-5>.
- Ugena, L., Hýřlová, A., Podlešáková, K., Humpfík, J.F., Doležal, K., Diego, N.D., Spíchal, L., 2018. Characterisation of biostimulant mode of action using novel multi-trait high-throughput screening of *Arabidopsis* germination and rosette growth. *Front Plant Sci* 9, 1327. <https://doi.org/10.3389/fpls.2018.01327>.
- Vrobel, O., Čavar Zeljković, S., Dehner, J., Spíchal, L., De Diego, N., Tarkowski, P., 2024. Multi-class plant hormone HILIC-MS/MS analysis coupled with high-throughput phenotyping to investigate plant–environment interactions. *Plant J* 129 (2), 818–832. <https://doi.org/10.1111/tpj.17010>.
- Walsh, J.J., Mangina, E., Negrão, S., 2024. Advancements in imaging sensors and AI for plant stress detection: a systematic literature review. *Plant Phenomics* 6, 0153. <https://doi.org/10.34133/plantphenomics.0153>.
- Wang, L., Wang, J., Liu, Z., Zhu, J., Qin, F., 2022. Evaluation of a deep-learning model for multispectral remote sensing of land use and crop classification. *Crop J* 10, 1435–1451. <https://doi.org/10.1016/j.cj.2022.01.009>.
- Wang, Y., Long, M., Wang, J., Gao, Z., Yu, P.S., 2017. PredRNN: recurrent neural networks for predictive learning using spatiotemporal LSTMs, in: *NIPS'17*. In: *Proceedings of the 31st International Conference on Neural Information Processing Systems*, pp. 879–888.
- Xin, X.-F., He, S.Y., 2013. *Pseudomonas syringae* pv. *tomato* DC3000: a model pathogen for probing disease susceptibility and hormone signaling in plants. *Annu Rev Phytopathol* 51, 473–498. <https://doi.org/10.1146/annurev-phyto-082712-102321>.
- Xu, X., Zhao, M., Shi, P., Ren, R., He, X., Wei, X., Yang, H., 2022. Crack detection and comparison study based on Faster R-CNN and Mask R-CNN. *Sensors* 22, 1215. <https://doi.org/10.3390/s22031215>.
- Yao, S., Lin, J., Bai, H., 2024. DPP: a novel disease progression prediction method for Ginkgo leaf disease based on image sequences. *Information* 15, 411. <https://doi.org/10.3390/info15070411>.
- Yuan, P., Xu, S., Zhai, Z., Xu, H., 2023. Research of intelligent reasoning system of *Arabidopsis thaliana* phenotype based on automated multi-task machine learning. *Front Plant Sci* 14. <https://doi.org/10.3389/fpls.2023.1048016>.
- Zafar, M., Amin, J., Sharif, M., Anjum, M.A., Mallah, G.A., Kadry, S., 2023. DeepLabv3++ based segmentation and best features selection using Slime Mould Algorithm for multi-class skin lesion classification. *Mathematics* 11, 364. <https://doi.org/10.3390/math11020364>.
- Zhai, Y., Zhou, L., Qi, H., Gao, P., Zhang, C., 2023. Application of visible/near-infrared spectroscopy and hyperspectral imaging with machine learning for high-throughput plant heavy metal stress phenotyping: a review. *Plant Phenomics* 5, 0124. <https://doi.org/10.34133/plantphenomics.0124>.
- Zhou, Z., Zhang, Y., Gu, Z., Yang, S.X., 2023. Deep learning approaches for object recognition in plant diseases: a review. *Intelligence & Robotics* 3, 514–537. <https://doi.org/10.20517/ir.2023.29>.